A High Frequency Isolated Current-fed Bidirectional DC/AC Converter for Grid-tied Energy Storage System

Xiaolei Hu, K.J. Tseng, Yitao Liu, Shan Yin and Mengqi Zhang
School of Electrical and Electronic Engineering
Nanyang Technological University,50 Nanyang Avenue ,Singapore 639798

***Abstract*— In applications of modern power distribution with distributed energy resources, grid-tied energy storage systems (ESS) will be increasingly incorporated. Energy storage devices (ESD) such as lithium-ion battery or super-capacitor cells however have low DC terminal voltages. It is essential to develop a bidirectional DC/AC converter to interface ESS based on low voltage cells to the higher voltage grid without using high number of cells in series. In this paper a bidirectional current-fed converter with high frequency transformer isolation is proposed. In this proposed topology, a current source inverter (CSI) is used to interface to the grid. A DC/DC converter with High frequency(HF) transformer is used to feed the current to CSI. Low voltage and high voltage side of DC/DC converter can be either Push-Pull or Full-Bridge. The proposed topology has the advantage of reduced component count and simple control strategy. Simulation and hardware results have shown that the proposed circuit can work in charging and discharging of the ESS and the control strategy is effective.**

Keywords—DC/DC, DC/AC, Current Source Inverter, High Frequency Link.

I. INTRODUCTION

Grid-tied energy storage system (ESS) is increasingly used in many power distribution applications such as uninterruptable power supplies (UPS) and solar photovoltaic power generation for buildings. Electrochemical battery which has acceptable power and energy density and super-capacitor which has high power density are commonly considered for the energy storage devices (ESD) inside the grid-tied ESS[1-3]. However terminal voltage of a single cell of either battery or super-capacitor is very low. There are basically two ways to interface the low terminal voltage ESD cells to the grid. One is to connect many cells in series to achieve a sufficiently high DC link voltage for a voltage source inverter (VSI) to interface the ESS to the grid. Due to varying chemical characteristics and aging effects, maintaining the many series-connected cells in balance is a major issue. For active balancing, auxiliary power electronic circuits known as cell equalizers [4, 5] are required to balance the series-connected cells. This will add to system complexity and cost.

Another way is to interface a low voltage ESS comprising only a few cells in series, to the high voltage AC grid by a converter with high-frequency (HF) transformer. As shown in Fig. 1, a bidirectional DC/DC converter with HF transformer such as dual active bridge (DAB) [6-9] converts the low voltage to a high-voltage DC link. A cascaded connected VSI allows bidirectional energy transfer between the grid and the DC link. This two-stage topology requires bulky DC capacitors and complex control strategy.

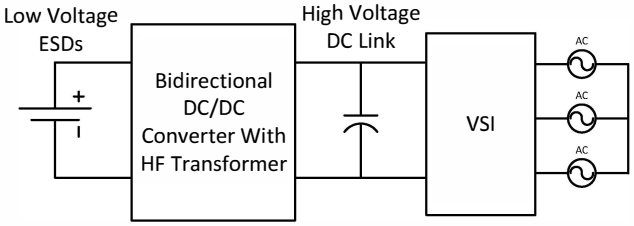

Fig. 1 Interfacing ESDs to grid with Bidirectional DC/DC cascaded by VSI

High frequency AC link (HFACL) [10, 11] as shown in Fig. 2 can be a candidate. However bidirectional switches are required. Furthermore the DC current of the ESD side cannot be regulated tightly.

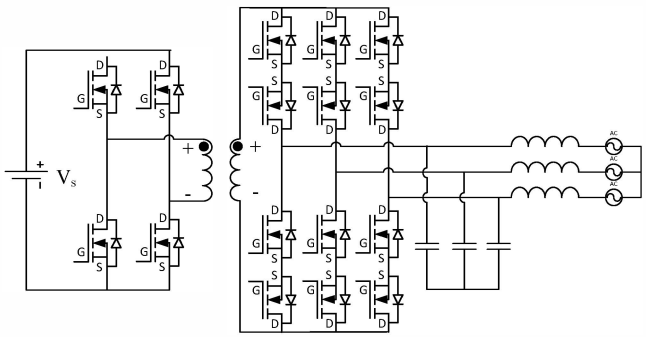

Fig. 2 Voltage-fed high frequency AC link

In this paper a novel bidirectional DC/AC converter with high frequency transformer isolation is proposed. The proposed topology has a current source inverter (CSI) to interface the grid. A DC/DC converter with either Push-Pull or Full-Bridge in low and high voltage side is used to feed the current to CSI. Contrary to conventional topology, current instead of voltage is fed from the low voltage to high voltage side. As the CSI works in boost mode, reduced transformer winding is required for the HF transformer. The proposed circuit also has a simple control strategy and a continuous ESS charging and discharging current. Section 2 will explain the operation of the

This research is funded by the Republic of Singapore's National Research Foundation through a grant to the Berkeley Education Alliance for Research in Singapore (BEARS) for the Singapore-Berkeley Building Efficiency and Sustainability in the Tropics (SinBerBEST) Program. BEARS has been established by the University of California, Berkeley as a center for intellectual excellence in research and education in Singapore.

proposed topology. Control strategy will be introduced in section 3. In section 4 and 5, simulation and hardware results will be presented to verify the proposed circuit.

II. Proposed Topology and Modulation Method

A. Proposed Toology

As shown in Fig. 3 (a), the proposed topology does not require bidirectional switch or bulky DC link capacitors. DC/DC part can be configured as Full-Bridge or Push-Pull as shown in Fig. 3 (b), (c), (d). The following of this paper will use Full-Bridge in low voltage side and Push-Pull in high voltage side to demonstrate the working principles and modulation of the proposed topology. ESD is connected to the primary winding of a HF transformer by a full-bridge. The two secondary windings of the HF transformer are connected to the inductor L_s by T_{21}, D_{21} and T_{22}, D_{21} respectively. A CSI connects Ls to the AC grid. GT_{1i} is the gate signals of T_{1i} (i□[1,4]). GT_{11} to GT_{14} have a fix duty cycle of 0.5 without considering dead time. GT_{11} (GT_{12}), GT_{13} (GT_{14}) are the same and GT_{11} (GT_{13}), GT_{12} (GT_{14}) are complementary. Phase shift of GT_{11} to GT_{12} is fixed at π. GT_{21} and GT_{22} are also complementary. CSI can regulate inductor current i_{L_s}, CSI with L_s can be modeled as a current source. Modulation of CSI and the coordination with DC/DC will be described in the next sub-section. Based on the power flow of ESD, the circuit has two

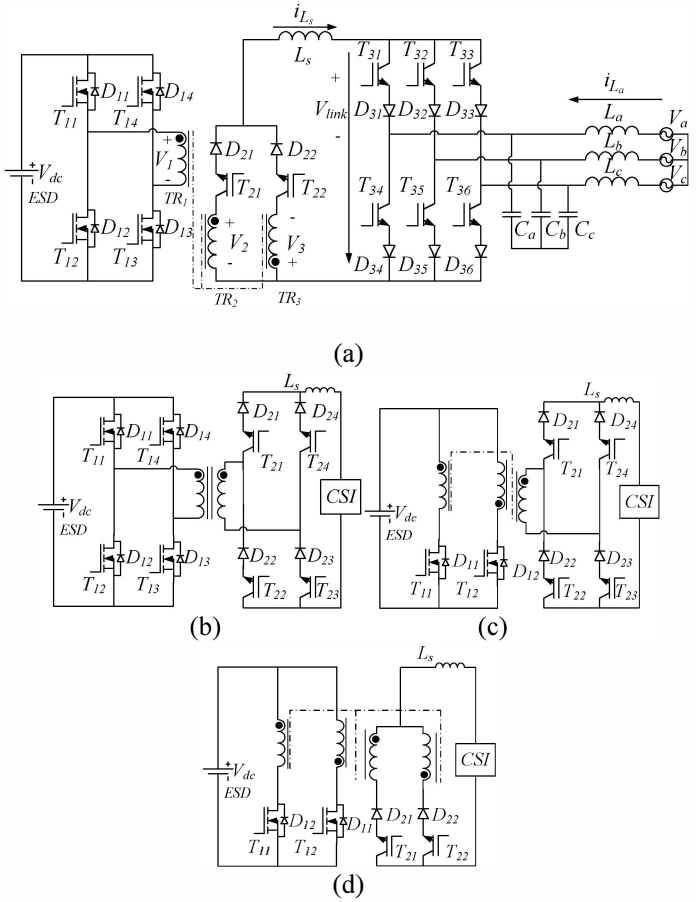

Fig. 3 Proposed Frequency Isolated Current-fed Bidirectional DC/AC Converter (a) Full-Bridge and Push-Pull (b) Full-Bridge and Full-Bridge (c) Push-Pull and Full-Bridge (d) Push-Pull and Push-Pull

operation modes: charging and discharging. Operation mode can be controlled by the phase shift of low voltage side switches and high voltage side switches of DC/DC part. This can be explained as follows. Assume that all the switches are ideal except for their body diodes. The dead time for voltage type converter and the shoot-through state for current type inverter are neglected.

Discharging Mode: In discharging mode, ESD is being discharged and energy is transferred from ESD to AC grid. Phase shift of T_{11} and T_{21} is controlled to 0 as shown in Fig. 4 (a). In this mode, the circuit has two operation stages:

Stage 1: As shown in Fig. 4 (b) T_{11} and T_{13} are turned on. V_{dc} is connected to TR_1, the primary winding of the HF transformer. Phase shift of T_{11} and T_{21} is 0, T_{21} is turned on while T_{22} is being blocked. TR_2 is connected to the current source I_s. Energy is being released from ESD.

Stage 2: T_{11} and T_{13} are turned off while T_{12} and T_{24} are turned on. $-V_{dc}$ is connected to TR_1, T_{22} is turned on while T_{21} is turned off. Energy is transferred from ESD to the gird.

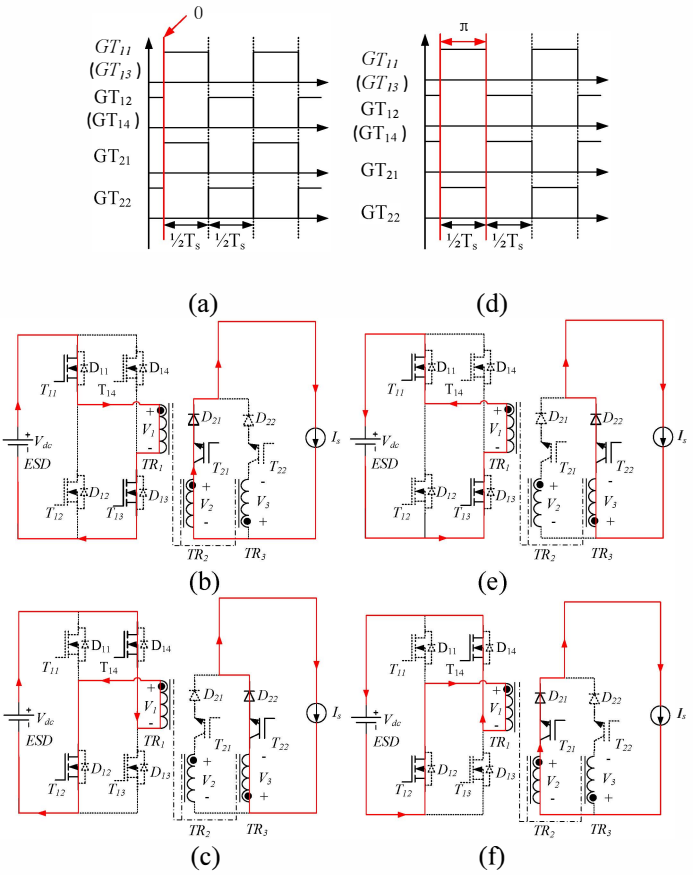

Fig. 4 Gate signals and circuit operation Stages for Discharging Mode: (a) Gate Signals, (b) Stage 1 (c) Stage 2 and Charging Mode: (d) Gate Signals, (e) Stage 3 (f) Stage 4.

Charging Mode: In Charging mode phase shift of T_{11} and T_{21} is controlled to be π. Gate signals are shown in Fig. 4 (d) and circuit operations stages are shown in Fig. 4 (e), (f). Stages of charging mode are described as follows.

Stage 3: T_{11} and T_{13} are turned on, V_{dc} is connected to TR_1, V_1 equals to V_{dc}. T_{22} is turned on while T_{21} is turned off. So V_3 equals to V_1 and ESD is charging by I_s.

Stage 4: T_{12} and T_{14} are turned on while T_{11} and T_{13} are turned off, $-V_{dc}$ is connected to TR_1 and V_1 equals to $-V_{dc}$. T_{22} is turned off and T_{21} is turned on. So V_2 equals to $-V_{dc}$ and ESD is charging by I_s.

B. Modulation Method

Space Vector Modulation (SVM) will be applied for controlling CSI. The hexagon of space vector definition is shown in Fig. 5. Switch group notation is ignored. E.g. S51 means T_{35} and T_{31} are turned on and group notation "3" is ignored.

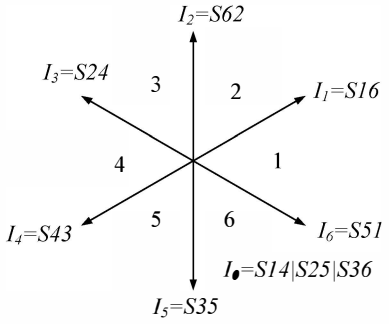

Fig. 5 Hexagon of CSI Space Vector

In order to keep volt-second balance for DC/DC side, DC modulation should be aligned with CSI modulation. Modulation for DC/DC and CSI in discharging mode is shown in Fig. 6.

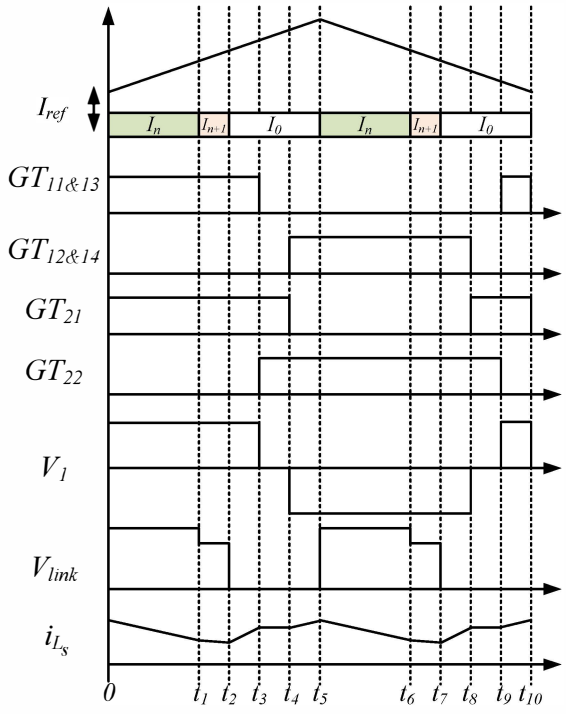

Fig. 6 Modulation and Key Waveforms in Discharging Mode

Fig. 6 shows a switching cycle for DC/DC Converter. Since current space vector depends on sectors, without loss of generality the following analysis will assume current space vector is in sector one and the grid voltage in dq frame has the same phase with current space vector without considering voltage drop on input AC inductor $L_{a,b,c}$. From *0* to t_1, Switches T_{11}, T_{13} and T_{21} is on. Since T_{35} and T_{31} are on, V_{link} equals to $V_{C_a} - V_{C_b}$. L_s is discharged by $V_1 - (V_{C_a} - V_{C_b})$ and its current is decreasing. From t_1 to t_2, T_{36} and T_{31} are on, V_{link} equals to $V_{C_a} - V_{C_c}$. L_s is discharged by $V_1 - (V_{C_a} - V_{C_c})$. While in null state of CSI which is from t_2 to t_5, DC/DC converter should turn off T_{11} and T_{13} while turn on T_{12} and T_{14}. At t3, when CSI has completely entered null sate, T_{11} and T_{13} are turned off. From t_3 to t_4 is the dead time duration for guaranteeing switches are turned off. At t_4, T_{12} and T_{14} are turned on. From t_4 to t_5, Ls is being charged by V_1. t_5 to t_{10} is the alternate half cycle and circuit operation is similar to that of t_1 to t_5.

Fig. 7 shows modulation method and key waveforms in charging mode. In charging mode, T_{11} to T_{14} work in synchronous rectifying mode to reduce conduction loss. Without considering the voltage drop on AC inductor $L_{a,b,c}$, gird voltage in dq frame has a phase difference of π with current reference. Without loss of generality, assuming current space vector is in sector one.

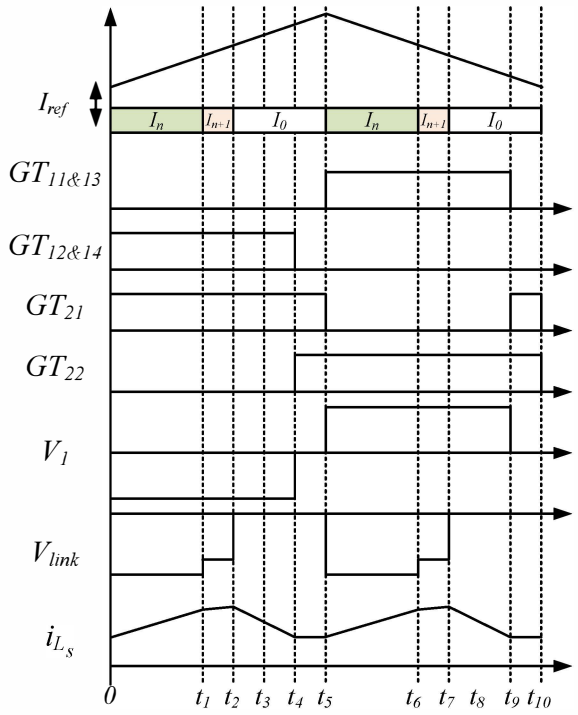

Fig. 7 Modulation and Key Waveforms in Charging Mode

From 0 to t_1, T_{35} and T_{31} are on, V_{link} equals to $V_{C_a} - V_{C_b}$. Since grid voltage in dq frame is shifted by π, V_{link} is negative. T_{12}, T_{14} and T_{21} are on, so inductor is being charged. While from t_2 to t_5, CSI is in null state and L_s is being discharged. At t_4, T_{12} and T_{14} are turned off. t_4 to t_5 is dead time to avoid short circuit V_{dc}. t_4 to t_5 is also used to ensure T_{22} is turned before T_{21} is turned off and providing a current path for inductor current.

III. CONTROL STRATEGY

As shown in Fig. 8, ESD current can be controlled by i_{L_s}, which is controlled by the CSI. Control and modulation of CSI is well stated in [12,13] .CSVM is the current source vector

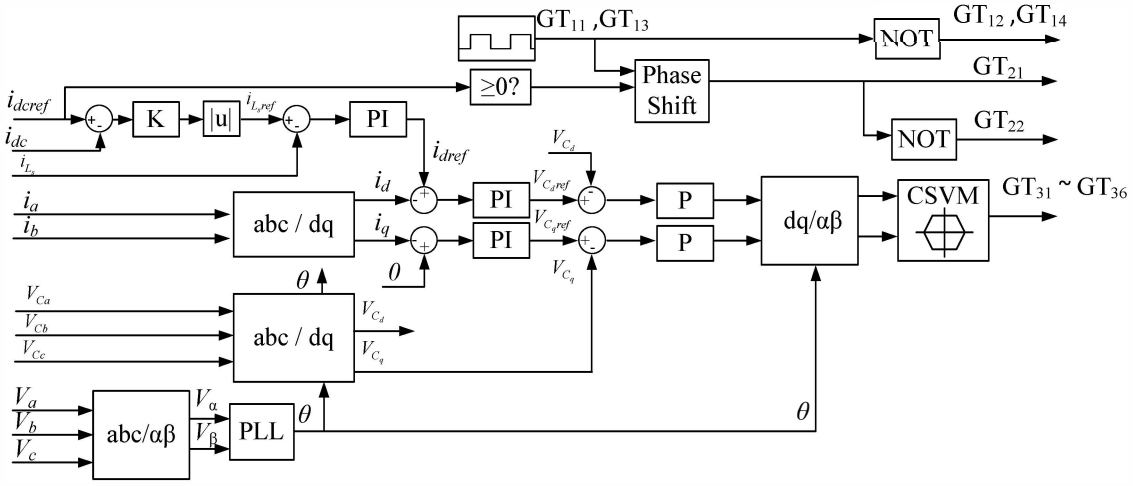

Fig. 8 System Control Diagram

generator that will generate the gate signals for the CSI switches. Charging and discharging is decided by the sign of the i_{dc} reference. Gate signals of GT_{11} and GT_{13} are square wave with 0.5 duty cycle. When i_{dcref} is greater than 0, system works in discharging mode. GT_{21} and GT_{11} are in phase. When i_{dcref} is negative, system is working in charging mode. GT_{11} will be shifted by π to get GT_{21}. This control strategy is easy to implement.

IV. Simulation Results

System parameters used for simulation are summarized in Table. I. A DC voltage source is used to simulate ESD.

Table. I Simulation System Parameters

V_{dc}	15V
$TR_1:TR_2:TR_3$	3:20:20
L_s	10mH
$L_{a,b,c}$	1mH
$C_{a,b,c}$	100μF
f_s	10kHz
$V_{a,b,c}(rms)$	115.5V
$i_{dc}ref$	66.7A

As shown in Fig. 9, the proposed circuit is working in discharging mode. In Fig. 9(a), when T_2 and T_4 are turned on, V_{dc} is applied at TR_1, V_2 and V_3 equals to $-V_{dc}$. T_5 is off and T_6 is on, so i_{TR_2} is 0 and i_{TR_3} equals to i_{L_s}. Energy is transferred from ESD through T_2, T_4 and T_6 to the grid. After half switching cycle T_1 and T_3 will be turned on, energy will be discharged from ESD through T_1, T_3 and T_5 to the grid. Fig. 9(b), (c) shows the grid voltage and current. Fig. 9(d) shows the ESD discharging current. Fig. 10 shows the circuit operation in charging mode. In Fig. 10(a), contrary to discharging mode, when T_2 and T_4 are turned on, T_5 is on and T_6 is off. Energy is transferred from the grid to ESD through T_5, T_2 and T_4. Voltage and current are shown in Fig. 10(b) and (c), ESD charging current is shown in Fig. 10(d). The simulation results show that the circuit can work in both charging and discharging mode properly and validates the theoretically analysis.

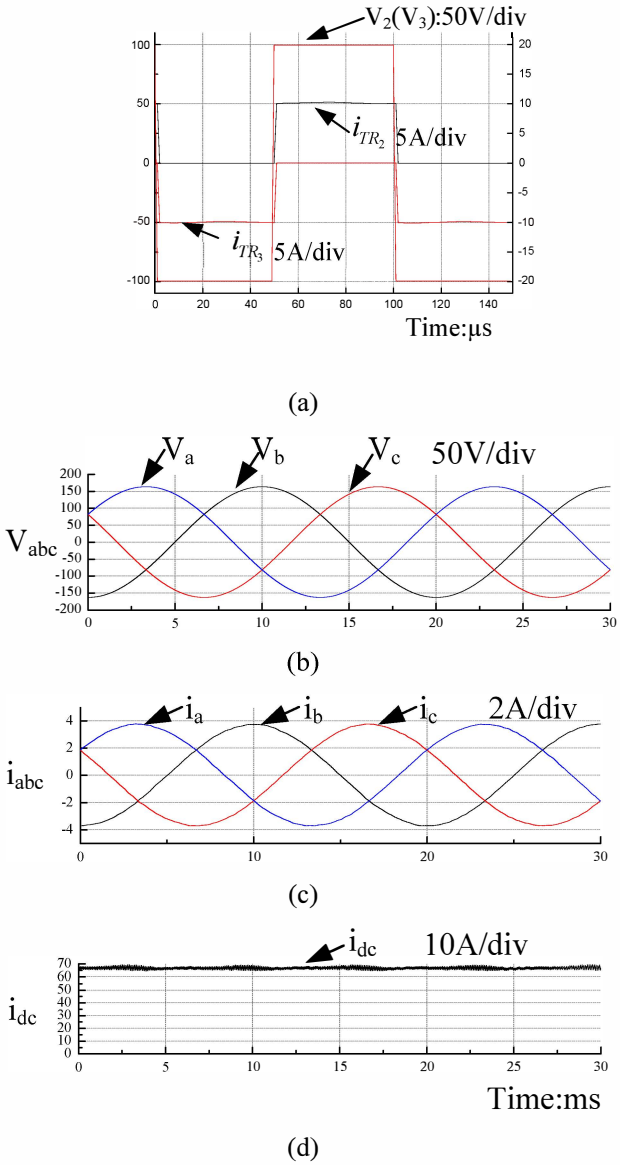

Fig. 9 Modulation and Key Waveforms in Discharging Mode

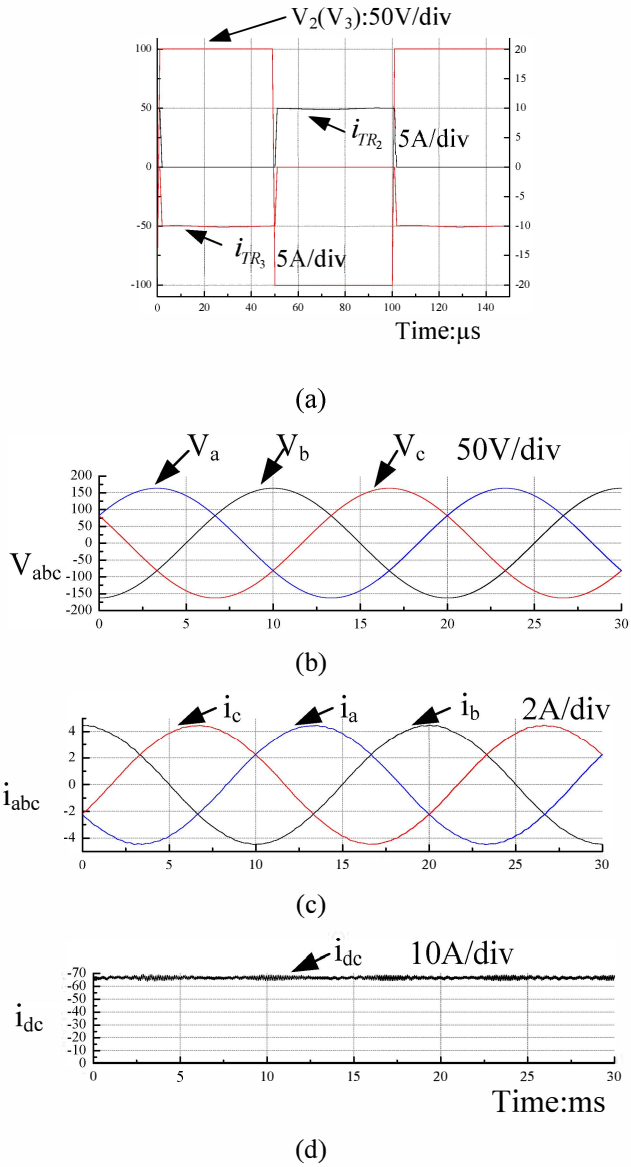

Fig. 10 Modulation and Key Waveforms in Discharging Mode

V. HARDWARE EXPERIMENTAL RESULTS

A hardware prototype shown as Fig. 11 has been built to verify the proposed topology and modulation method. DC/DC side of this prototype is based on full-bridge and full-bridge which is shown in Fig. 3 (b).

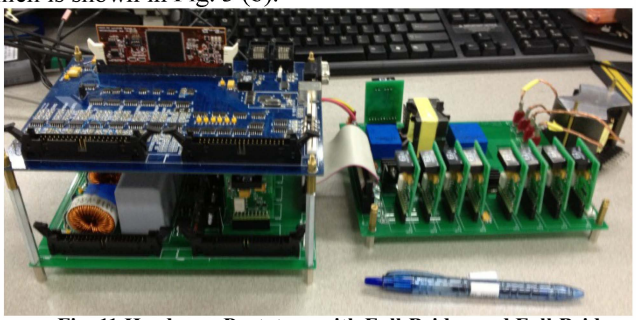

Fig. 11 Hardware Prototype with Full-Bridge and Full-Bridge Configuration

System parameters used for discharge mode is summarized in Table II.

Table. II System Parameters for Discharge Mode

V_{dc}	50V
$TR_1:TR_2$	1:3
L_s	0.5mH
$L_{a,b,c}$	0.3mH
$C_{a,b,c}$	20μF
f_s	20kHz
$V_{a,b,c}(rms)$	100V
$i_{dc}ref$	2.5A

Key waveforms of discharge mode are shown in Fig. 12.

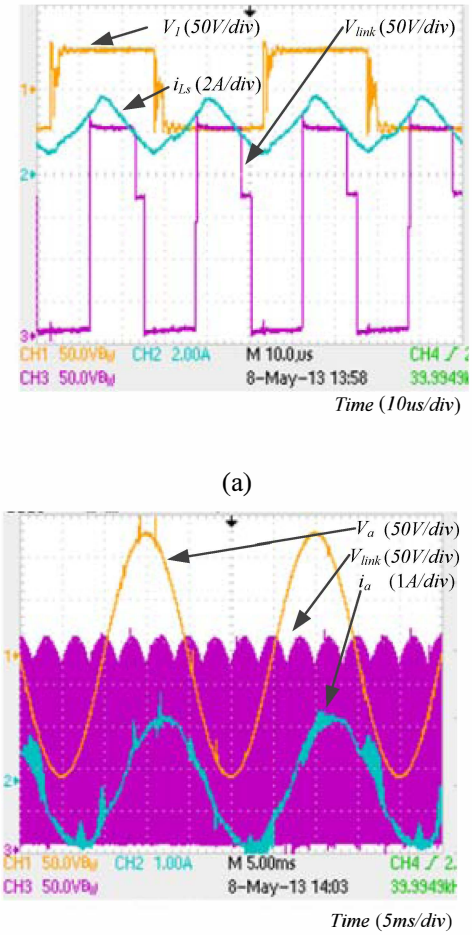

Fig. 12 Waveforms in Discharge Mode (a) Low voltage side transformer and link voltage, inductor current (b) input Ac voltage and current with link voltage

In discharge mode, energy is transferred from DC side to AC side. In this mode, ESD will be discharged and release energy to AC grid. As shown in Fig. 12 (a), V_1 is the voltage of primary side of the high frequency transformer. V_{link} is the virtual DC link voltage as shown in Fig. 3(a). V_{link} is not a constant voltage as the case of VSI and is decided by input AC voltage and modulation method. After applied modulation method shown as Fig. 6, a balanced primary side voltage is

applied. In Fig. 12 (b), input AC voltage and current are shown. There is a small phase difference between the voltage and current. So power factor is not unit. This phase difference is due to the LC filter and power factor can be compensated to unit which will be done in the future.

Key waveforms of charge mode are shown in Fig. 13. DC voltage is changed to 35V, other parameters are the same as discharge mode.

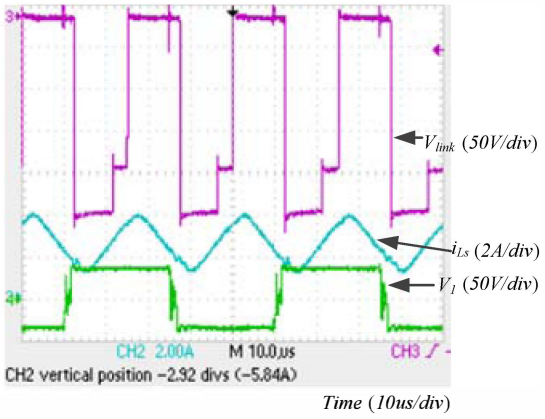

(a)

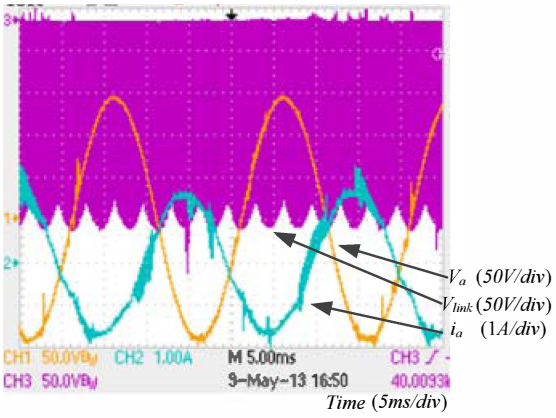

(b)

Fig. 13 Waveforms in Discharge Mode (a) Low voltage side transformer and link voltage, inductor current (b) input Ac voltage and current with link voltage

In charge mode, energy is transferred from AC side to DC side. In this mode, ESD will be charged by AC grid. As shown in Fig. 13(a), V_{link} is reversed and inductor current is not reversed. A square wave is got at the low voltage side and is rectified to charge V_{dc}. As shown in Fig. 13 (b), AC voltage and current has a phase difference close to π and is charging V_{dc}

VI. CONCLUSION

In this paper a current-fed bidirectional DC/AC converter with HF transformer isolation is proposed to interface low voltage ESDs such as batteries and super-capacitors to AC grid. The proposed topology is comprised of a CSI, a DC/DC converter with a HF transformer. DC/DC converter for low voltage side and high voltage side can be either push-pull or full-bridge. Current instead of voltage is fed from the high voltage side to the low voltage. CSI is used to regulate the inductor current that will be fed to the low voltage side. CSI works in boost mode and reduced low voltage side transformer winding is required. The proposed circuit has the advantage of simple control strategy and fewer components. Simulation results have proven that the proposed circuit worked properly in both charging and discharging modes and the control strategy is effective. It can thus avoid the balancing issues associated with ESS which relies on high number of cells in series.

REFERENCES

[1] Y. Chen and K. Smedley, "Three-Phase Boost-Type Grid-Connected Inverter," IEEE Trans. Power Electron., vol. 23, pp. 2301-2309, 2008.

[2] B. Mirafzal, M. Saghaleini, and A. K. Kaviani, "An SVPWM-Based Switching Pattern for Stand-Alone and Grid-Connected Three-Phase Single-Stage Boost Inverters," IEEE Trans. Power Electron., vol. 26, pp. 1102-1111, 2011.

[3] Z. Qin, D. Sha, and X. Liao, "A three-phase boost-type grid-connected inverter based on synchronous reference frame control," in Applied Power Electronics Conference and Exposition (APEC), 2012 Twenty-Seventh Annual IEEE, 2012, pp. 384-388.

[4] K. Chol-Ho, K. Moon-Young, P. Hong-Sun, and M. Gun-Woo, "A Modularized Two-Stage Charge Equalizer With Cell Selection Switches for Series-Connected Lithium-Ion Battery String in an HEV," IEEE Trans. Power Electron., vol. 27, pp. 3764-3774, 2012.

[5] H.-S. Park, C.-H. Kim, K.-B. Park, G.-W. Moon, and J.-H. Lee, "Design of a Charge Equalizer Based on Battery Modularization," Vehicular Technology, IEEE Transactions on, vol. 58, pp. 3216-3223, 2009.

[6] F. Krismer and J. W. Kolar, "Closed Form Solution for Minimum Conduction Loss Modulation of DAB Converters," IEEE Trans. Power Electron., vol. 27, pp. 174-188, 2012.

[7] F. Krismer and J. W. Kolar, "Efficiency-Optimized High-Current Dual Active Bridge Converter for Automotive Applications," IEEE Trans. Ind. Electron., vol. 59, pp. 2745-2760, 2012.

[8] F. Krismer and J. W. Kolar, "Accurate Power Loss Model Derivation of a High-Current Dual Active Bridge Converter for an Automotive Application," IEEE Trans. Ind. Electron., vol. 57, pp. 881-891, 2010.

[9] H. Bai and C. Mi, "Eliminate Reactive Power and Increase System Efficiency of Isolated Bidirectional Dual-Active-Bridge DC/DC Converters Using Novel Dual-Phase-Shift Control," IEEE Trans. Power Electron., vol. 23, pp. 2905-2914, 2008.

[10] D. Chen and Y. Chen, "Step-up AC Voltage Regulators with High-Frequency Link," IEEE Trans. Power Electron., vol. 28, pp. 390-397, 2013.

[11] D. Sha, K. Deng, Z. Guo, and X. Liao, "Control Strategy for Input-Series/Output-Parallel High-Frequency AC Link Inverters," IEEE Trans. Ind. Electron., vol. 59, pp. 4101-4111, 2012.

[12] S. A. S. Grogan, D. G. Holmes, and B. P. McGrath, "High-Performance Voltage Regulation of Current Source Inverters," IEEE Trans. Power Electron., vol. 26, pp. 2439-2448, 2011.

[13] D. N. Zmood and D. G. Holmes, "Improved voltage regulation for current-source inverters," IEEE Trans. Ind. Appl., vol. 37, pp. 1028-1036, 2001.